iScience

CellPress
OPEN ACCESS

Article

Risk model based on minichromosome maintenance 2 using objective assessment for predicting survival of neuroblastoma

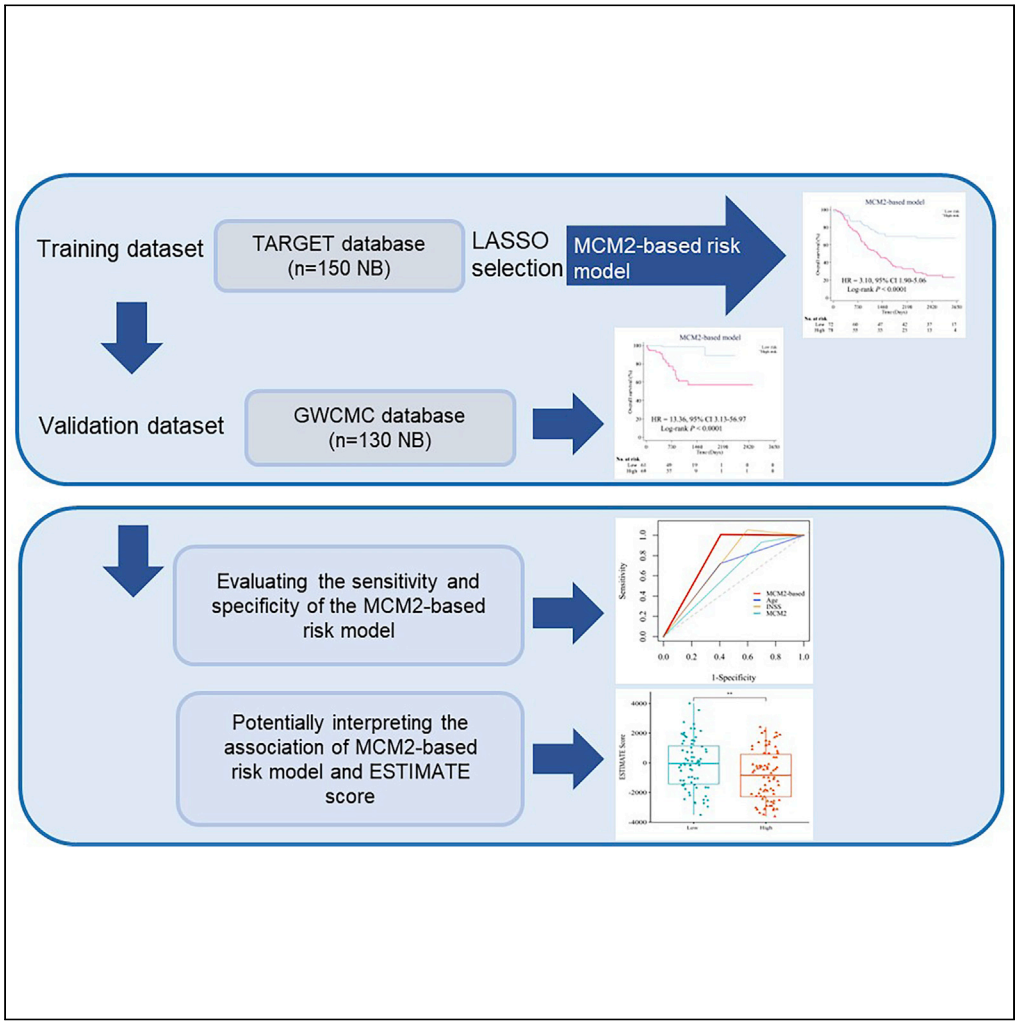

Liang Zeng, Xiao-Yun Liu, Lei Miao, ..., Kai Liu, Jiahao Feng, Hai-Yun Wang

zlxx03@126.com (L.Z.)
wanghy29@mail3.sysu.edu.cn (H.-Y.W.)

Highlights

A MCM2 expression, age, and INSS are composed of a risk model for prognosis

A MCM2-based risk model better predicts NB patient survival than each factor alone

The MCM2-based risk model potentially influences infiltration of immune cells

Zeng et al., iScience 26, 105974
February 17, 2023
https://doi.org/10.1016/j.isci.2023.105974

iScience

CellPress
OPEN ACCESS

Article

Risk model based on minichromosome maintenance 2 using objective assessment for predicting survival of neuroblastoma

Liang Zeng,[1,5,*] Xiao-Yun Liu,[2,5] Lei Miao,[3,5] Kai Chen,[1] Hui Xu,[1] Liang-Jun Qin,[1] Meng Li,[3] Kai Liu,[4] Jiahao Feng,[4] and Hai-Yun Wang[1,3,6,*]

SUMMARY

Aberrant minichromosome maintenance (MCM) expression is associated with tumorigenesis. Here, we performed immunohistochemistry integrated with digital pathology to identify MCM2/5/6 expression in 130 neuroblastoma patients. A risk score was established using least absolute shrinkage and selection operator that predicts outcomes according to MCM2 expression, age, and the International Neuroblastoma Staging System in the Therapeutically Applicable Research to Generate Effective Treatments (TARGET) dataset (n = 150), where the patients with high risk had significantly worse prognosis that was validated in a hospital-based cohort (n = 130). After multivariable adjustment, the risk model remained an independent factor for survival in the TARGET cohort (overall survival [OS]: hazard ratio [HR] 2.3, 95% confidence interval [CI] 1.4–4.0; event-free survival [EFS]: HR 1.8, 95% CI 1.1–3.1) and for OS in the validation cohort (HR 8.3, 95% CI 1.6–44.5). The ESTIMATE indicates that the risk model is negatively correlated with low ESTIMATE and stromal scores. These findings show the additive nature of this score, fostering its future implementation with new prognostic variables.

INTRODUCTION

Neuroblastoma (NB), an embryonal tumor, arises in the neuroectoderm and accounts for approximately 15% of all cancer-related deaths in the pediatric population.[1] The heterogeneous biology of NB commonly manifests as diverse clinical presentations and courses ranging from spontaneous regression to life-threatening metastasizing progression, even at the same clinical stage and with the application of intensive therapy.[2] Moreover, there is a high frequency of metastatic disease at the time of diagnosis. Despite multimodal anticancer therapies implemented in clinics combining surgery with chemotherapy, radiotherapy, and anti-disialoganglioside (GD2) *monoclonal antibody* (mAb)-based immunotherapy, overall survival rates remain quite abysmal, especially for NB patients with high-risk disease defined by clinical factors and tumor biology associated with relapse/metastasis, with a poor survival of approximately 50% at 5 years[3,4] To date, the current risk classification is limited by spatiotemporal heterogeneity, and optimal biomarkers are urgently needed. Thus, identifying reliable biomarkers for optimizing the prognosis and informing treatment strategies in the future is imperative.

The minichromosome maintenance (MCM) complex consists of six highly conserved proteins (MCM2–7) that interact to form a hexamer[5] and directly plays a considerable role in the initiation of DNA replication. MCMs are expressed only during the cell cycle and are therefore considered useful as proliferation markers. Not surprisingly, dysregulation of MCM expression is observed in many human cancers[5,6] and has been identified as being associated with carcinogenesis. For example, patients with oral squamous cell carcinoma[7] and cervical carcinoma[8] have increased expression of MCM2. In addition, MCM4 and MCM7 are reported to be better biomarkers than Ki-67 for esophageal adenocarcinoma and precancerous lesions. Another study showed that deregulated MCM7 expression may actively contribute to tumor formation, progression, and malignant conversion.[9]

Nevertheless, there are few investigations on the prognostic value of the MCM complex for NB patients. Accordingly, we first constructed a prognostic risk model using the Therapeutically Applicable Research to Generate Effective Treatments (TARGET) dataset and validated it using our dataset, whereby the

[1]Department of Pathology, Guangzhou Institute of Pediatrics, Guangzhou Women and Children's Medical Center, Guangzhou Medical University, Guangdong Provincial Clinical Research Center for Child Health, National Children's Medical Center for South Central Region, No. 9 Jinsui Road, Guangzhou 510623, People's Republic of China

[2]Department of Molecular Diagnostics, Sun Yat-Sen University Cancer Center, State Key Laboratory of Oncology in South China, Collaborative Innovation Center for Cancer Medicine, Guangzhou 510060, People's Republic of China

[3]Department of Pediatric Surgery, Guangzhou Institute of Pediatrics, Guangdong Provincial Key Laboratory of Research in Structural Birth Defect Disease, Guangzhou Women and Children's Medical Center, Guangzhou Medical University, Guangdong Provincial Clinical Research Center for Child Health, National Children's Medical Center for South Central Region, Guangzhou 510623, People's Republic of China

[4]Cells Vision (Guangzhou) Medical Technology Inc., Guangzhou 510320, People's Republic of China

[5]These authors contributed equally

[6]Lead contact

*Correspondence: zlxx03@126.com (L.Z.), wanghy29@mail3.sysu.edu.cn (H.-Y.W.)

https://doi.org/10.1016/j.isci.2023.105974

Table 1. Clinicopathological characteristics of neuroblastoma patients in the GWCMC cohort

Variable	All cases (n = 130)
Age, months	
<18	69 (53.1)
≥18	61 (46.9)
Sex	
Female	58 (44.6)
Male	72 (55.4)
Pathological grade	
Well differentiated	23 (17.7)
Undifferentiated or poorly differentiated	102 (78.4)
Unknown	5 (3.9)
MKI	
Low	66 (50.8)
Intermediate	13 (10.0)
High	35 (26.9)
Unknown	16 (12.3)
MYCN	
Nonamplified	116 (89.2)
Amplified	14 (10.8)
INSS[a]	
Early stage	40 (30.8)
Advanced stage	90 (69.2)
COG risk group	
Low	40 (30.8)
Intermediate	34 (26.2)
High	56 (43.0)
3-year OS (95% CI)	79.5% (70.4%–86.1%)
3-year EFS (95% CI)	57.8% (47.9%–66.5%)
5-year OS (95% CI)	73.1% (59.3%–82.9%)
5-year EFSS (95% CI)	52.3% (40.1%–63.1%)

MKI, mitosis-karyorrhexis index; MYCN, encoding the transcription factor N-MYC; INSS, the International Neuroblastoma Staging System; COG, Children's Oncology Group; OS, overall survival; EFS, event-free survival; CI, confidence interval; GWCMC, Guangzhou Women and Children's Medical Center.
[a]INSS stage 1, 2, and 4s as the early stage; INSS stage 3 and 4 as the advanced stage.

expression of MCM2/5/6 based on digital pathology was analyzed in a large sample of 130 NB patients to assess NB patient overall survival (OS) and event-free survival (EFS). Then, we explored the relationship between the prognostic risk model and the *Estimation of STromal and Immune cells in MAlignant Tumor tissues using Expression data* (ESTIMATE) score in NB, which may provide more information for developing a risk model capable of prognostication and a new clue for the targeted immunotherapy.

RESULTS

Patient characteristics

A total of 130 NB patients were enrolled in this study. The 3-year OS and EFS were 79.8% (70.8–86.3%) and 57.7% (47.9–66.3%), respectively, and the 5-year OS and EFS were 73.3% (59.5–83.1%) and 52.1% (40.0–63.0%), respectively, in the 130 NB patients. All patients were followed up (median: 910 days, range: 18–3047 days). Clinical features, including age, sex, International Neuroblastoma Staging System (INSS), and the Children's Oncology Group (COG), are summarized in Table 1.

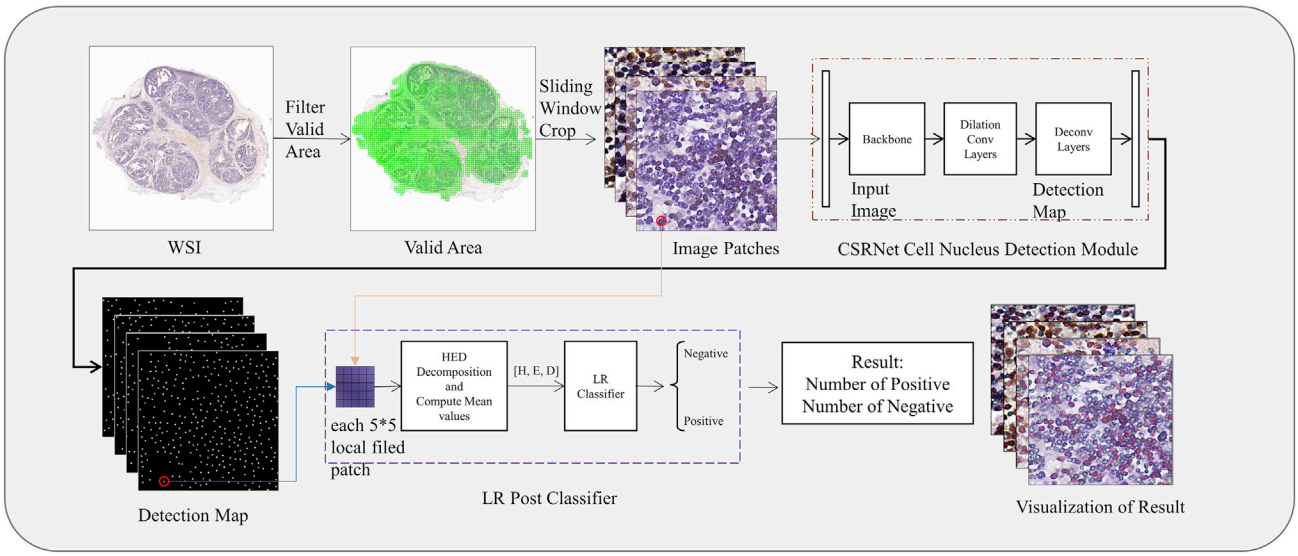

Figure 1. Framework of the automated cell nucleus counting system for MCM2/5/6

The expression of MCM2/5/6

MCM2/5/6 are expressed in the nucleus of tumor cells, and all pathological images were autoexamined using computational image analysis. The design of the automated cell nucleus counting system is as follows (Figure 1). Representative images of immunohistochemistry (IHC) staining for MCM2/5/6 are shown in Figure S1. Based on computational pathology analysis, the expression of the three biomarkers was digitally defined and quantified as the percentage of the positive expression accounting for all negative and positive nuclear expression within effective areas (per mm^2). The expression of MCM2/5/6 with the median percentage calculated in NB tissues according to the early and advanced stage[10] is summarized in Figure S2. Specifically, the highest expression was found for MCM6 (median: 39.2%, 95% CI: 33.9%–43.5%/mm^2), followed by MCM2 (median: 21.6%, 95% CI: 17.8%–25.7%/mm^2) and MCM5 (median: 4.7%, 95% CI: 3.3%–6.1%/mm^2). We also analyzed the relationship between the expression of these three biomarkers and clinical features, such as INSS, encoding the transcription factor N-MYC (MYCN) status, COG risk classification, and pathological grade, showing that there was no relationship between them (Table S1).

Prognostic value of each marker

We next explored the prognostic value of the markers MCM2/5/6 in NB patients. In the TARGET dataset, high expression of MCM2/5/6 was associated with a higher risk of death (HR 2.70, 95% CI 1.61–4.55, p = 0.0001, Figure 2A; HR 1.96, 95% CI 1.18–3.28, p = 0.0115; Figure 2B; HR 2.04, 95% CI 1.10–3.78, p = 0.0244; Figure 2C), although similar results were found only for the risk of any event in NB patients with high expression of MCM2 and MCM6 (Figures 2 D and 2F). In the Guangzhou Women and Children's Medical Center (GWCMC) dataset, high expression of MCM2 was associated only with inferior OS (HR 8.27, 95% CI 1.11–61.31, p = 0.0036, Figure 3A).

The combined prognostic effect of MCM2, age, and INSS

To develop a more sensitive model to predict NB prognosis, we constructed a prognostic score model significantly associated with OS using penalized least absolute shrinkage and selection operator (LASSO) Cox regression models (Figure S3). A risk score was then calculated for each patient using a formula that included MCM2, age, and INSS weighted by their regression coefficient as follows: risk score = (2.2814 x percentage of MCM2 positive expression) + (1.0258 x age) + (2.465 x INSS).

Based on the median prediction probability of the risk score, we classified 72 NB patients in the TARGET dataset into a low-risk group and 78 NB patients into a high-risk group. The clinicopathological characteristics of the patients stratified with the MCM2-based risk model are summarized in Table S2. The high-risk

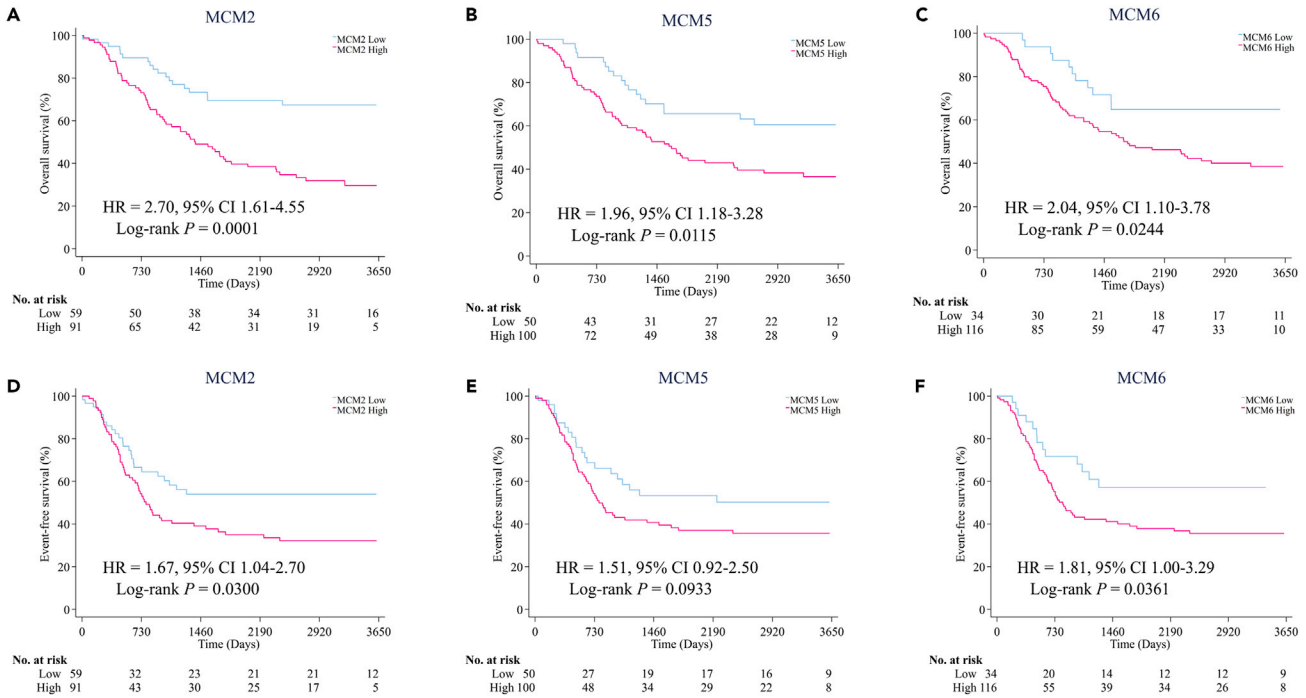

Figure 2. Kaplan-Meier curves for OS and EFS according to the expression levels of MCM2/5/6 in the TARGET dataset (n = 150)

(A–F) Plots for OS show (A) MCM2, (B) MCM5, and (C) MCM6 in NB patients. Plots for EFS show (D) MCM2, (E) MCM5, and (F) MCM6 in NB patients. OS, overall survival; EFS, event-free survival; HR, hazard ratio; CI, confidence interval; MCM, minichromosome maintenance; NB, neuroblastoma.

group had a shorter OS than the low-risk group (HR 3.10, 95% CI 1.90–5.06, p < 0.0001, Figure 4A), as well as an unfavorable EFS (HR 2.08, 95% CI 1.31–3.31, p = 0.0015, Figure 4B).

To determine whether the model has similar prognostic value, we applied it to the GWCMC cohort of 130 NB patients and classified them into low-risk (n = 61) and high-risk (n = 69) groups. Again, the high-risk group had a shorter OS (HR 13.36, 95% CI 3.13–56.97, p < 0.0001, Figure 4C) and an unfavorable EFS (HR 3.01, 95% CI 1.62–5.59, p = 0.0002, Figure 4D). The 3- and 5-year OS and EFS rates in each group and the number of patients in each group who had an event are listed in Tables S2 and S3, respectively.

Furthermore, we calculated the cumulative risk score for each patient and used receiver operating characteristic (ROC) analysis to compare the sensitivity and specificity of the MCM2-based prognostic risk model with age, INSS, and MCM2 alone (Figure S4). The MCM2-based risk model showed significantly better prognostic value than the INSS alone for OS (area under the ROC curve [AUROC] 0.82 [95% CI 0.74–0.90] vs. 0.77 [0.70–0.84]) but not for EFS (0.77 [95% CI 0.68–0.86] vs. 0.78 [0.70–0.86]). At the same time, the calibration plots of the MCM2-based risk model for the probability of 3- or 5-year OS showed optimal agreement between the prediction by the model and the actual observation in the TARGET and GWCMC datasets, respectively (Figure 5). This suggests that the MCM2-based prognostic model might provide more biological information for predicting OS in NB patients.

After multivariable adjustment by clinicopathological risk factors, such as age and INSS, the MCM2-based risk model remained a powerful and independent prognostic factor for OS and EFS in the TARGET cohort (OS: HR 2.3, 95% CI 1.4–4.0, p = 0.002; EFS: HR 1.8, 95% CI 1.1–3.1, p = 0.026; Table 2) and for OS in the GWCMC cohort (HR 8.3, 95% CI 1.6–44.5, p = 0.013; Table 2).

Relationship of the MCM2-based risk model with ESTIMATE score

To explore the potential mechanisms by which the risk model is capable of predicting patient survival, we performed ESTIMATE analysis and assessed the infiltration of immune cells in the TARGET dataset. Lower scores in both ESTIMATE (Figure 6A, p < 0.001) and stromal (Figure 6B, p < 0.0001) analyses were significantly associated with the high-risk group stratified by the MCM2-based risk model compared with the

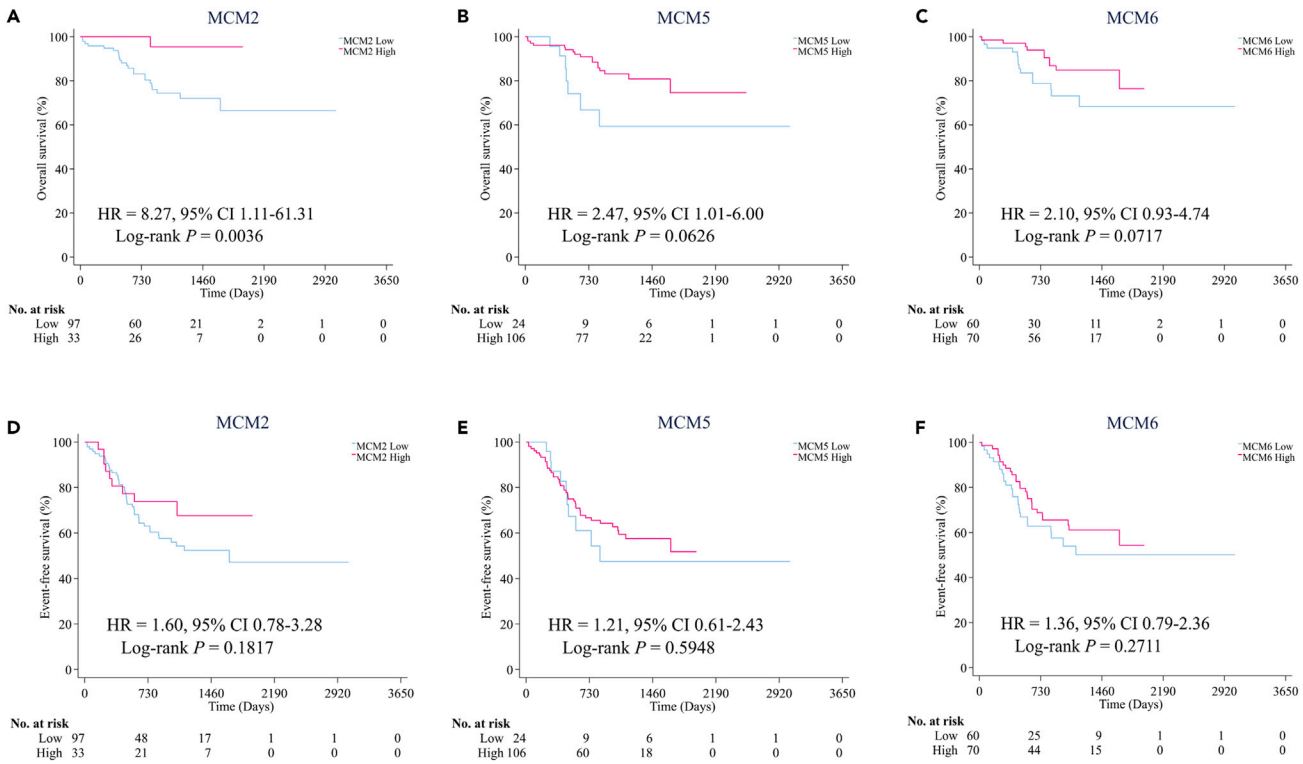

Figure 3. Kaplan-Meier curves for OS and EFS according to the expression levels of MCM2/5/6 in the GWCMC dataset (n = 130)

(A–F) Plots for OS show (A) MCM2, (B) MCM5, and (C) MCM6 in NB patients. Plots for EFS show (D) MCM2, (E) MCM5, and (F) MCM6 in NB patients. OS, overall survival; EFS, event-free survival; HR, hazard ratio; CI, confidence interval; MCM, minichromosome maintenance; NB, neuroblastoma.

low-risk group. Not surprisingly, we also observed a similar phenomenon when analyzing the immune score, even though there was no significant difference (Figure 6C). Survival analyses indicated that low ESTIMATE and immune scores were significantly associated with worse OS, with p values of 0.022 and 0.016, respectively (Figures 6D and 6F), and low stromal scores were marginally associated with worse OS (Figure 6E, p = 0.065). Overall, the NB patients with high risk stratified by the MCM2-based risk model had a worse OS, potentially due to lower infiltration of immune cells.

DISCUSSION

In this study, we used current RNA sequencing data combined with our hospital-based dataset to explore MCM2/5/6 expression levels in NB patients. We show that our MCM2-based risk model was well developed and has good performance in predicting NB patient OS and EFS. Our observations suggest that gene expression, especially MCM2 gene expression, may add more information to traditional clinical risk factors, such as age and INSS, in terms of prognostication, offering a potential target for clinical therapeutics.

A meta-analysis reported that MCM2 was associated with worse outcomes in human cancer,[11] and exogeneous overexpression of MCM2 increased anchorage-independent cell growth, resulting in cell migration and invasion in medulloblastoma.[12] More interestingly, only MCM2 expression remained an independent adverse factor for prognosis in multiple myeloma, even though MCM2/3/4/6/8 expression levels were simultaneously detected, indicating that MCM2 may be a strong therapeutic target for this disease.[13] Another study found that MCM2 overexpression in tumors harboring tumor protein 53 (TP53) mutation was a risk factor for poor prognosis.[14] Alternatively, MCM2 is usually considered a proliferation marker, and it seemed to outperform Ki-67 as a tool to assess cellular proliferation in a large cohort of patients diagnosed with breast cancer.[15] A recent study reported that MCM2 overexpression is associated with tumor growth in an NB xenograft mouse model and that inhibition of MCM2 significantly increases cisplatin activity, supporting MCM2 as a target for NB therapy.[16] It was reported that knockdown of MCM2 in NB cell lines suppressed cell growth.[17] Taken together, these findings suggest that MCM2 expression mainly promotes tumor growth across cancer types. In line with previous studies, we found that a MCM2-based risk

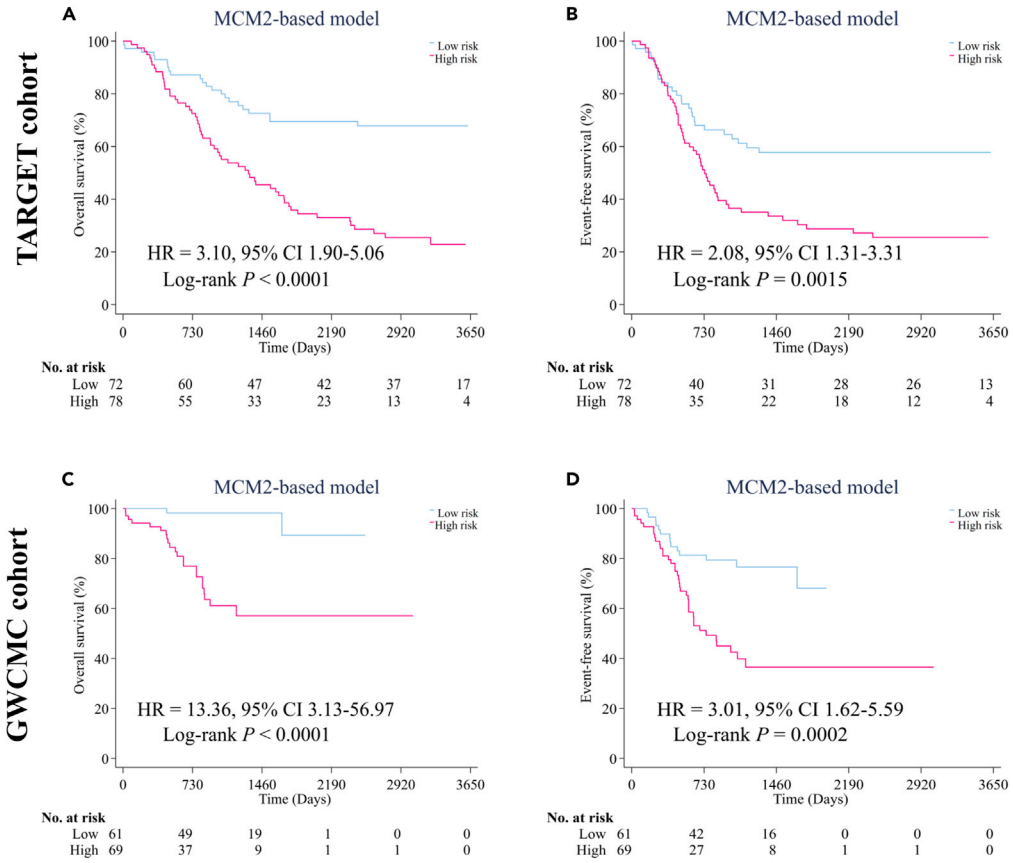

Figure 4. Kaplan-Meier survival estimates of the MCM2-based risk model for predicting NB patient survival

(A–D) Plots for OS are shown in (A) and those for EFS are shown in (B) for the TARGET dataset according to the MCM2-based risk model; similarly, plots for OS are shown in (C) and those for EFS are shown in (D) for the GWCMC dataset according to the MCM2-based risk model.

OS, overall survival; EFS, event-free survival; HR, hazard ratio; CI, confidence interval; MCM, minichromosome maintenance; NB, neuroblastoma.

model predicts poor OS and EFS in two cohorts; importantly, the risk model was somewhat associated with tumor microenvironment, which might provide a potential target for immune therapy in NB.

It is well known that the tumor microenvironment is both diverse and complex as different immune cells are capable of infiltrating tumor tissues, indicating that the synergistic interaction of different immune cells and tumor cells might provide a better understanding of tumorigenesis. The ESTIMATE algorithm was applied to calculate the ESTIMATE, stromal, and immune scores,[18] and the results implied that infiltrating stromal and immune cells existed in tumor tissues. Accordingly, we analyzed the relationship between immune cell infiltration and the MCM2-based risk model, which would explain the underlying mechanisms of the MCM2-based risk model in predicting clinical outcomes. Remarkably, we found that high ESTIMATE, stromal, and immune scores were significantly/marginally associated with better OS in NB patients. These findings are consistent with those of previous studies.[19,20] Furthermore, we explored the relationship between the MCM2-based model and ESTIMATE score and found that a high-risk score in the MCM2-based risk model was significantly correlated with low ESTIMATE and stromal scores. Not surprisingly, it was observed that a lower immune score tended to be associated with a high-risk score. Several studies have recently reported that MCM2 expression could affect the immune cell infiltration. For example, an analysis of The Cancer Genome Atlas data recently revealed that MCM2 is not only significantly upregulated as a component of the tumor mutation burden, which is commonly used as a biomarker for cancer immunotherapy,[21] in advanced stages of almost all cancers but also closely associated with the infiltration of various immune cells in melanoma[22] and hepatocellular carcinoma.[23] Overall, it was expected that the interplay of MCM2 expression and tumor microenvironment critically affects tumor evolution, which subsequently

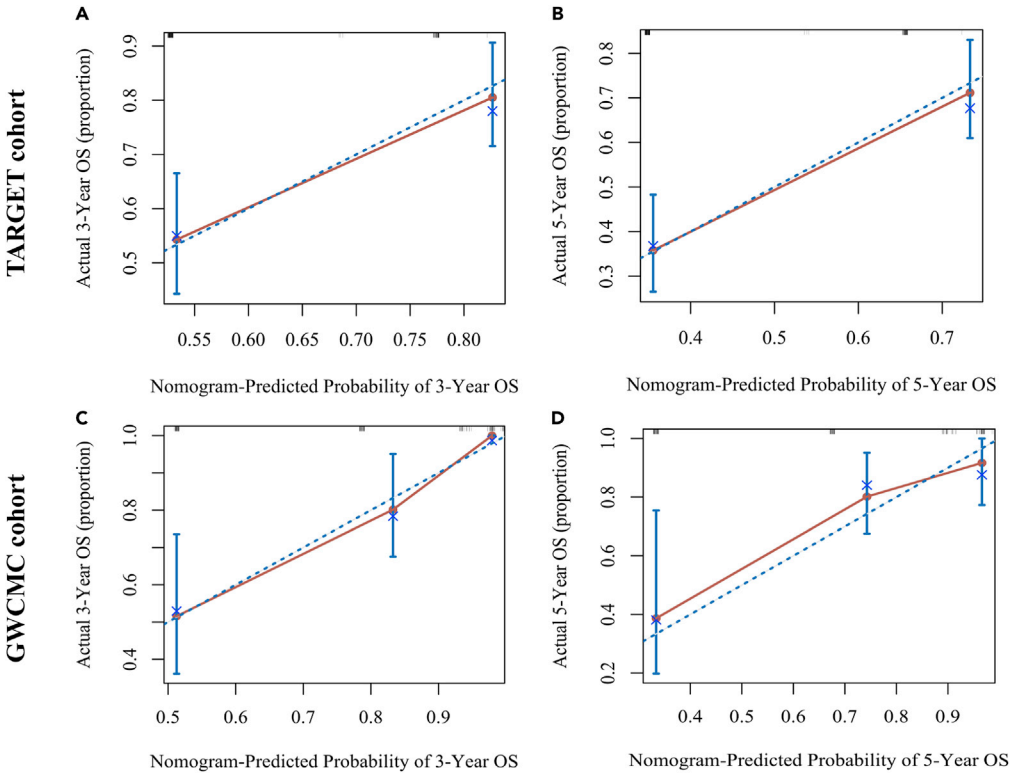

Figure 5. Calibration plots of the MCM2-based risk model for predicting 3- and 5-year OS in patients from the TARGET (A and B) and GWCMC (C and D) datasets, respectively

OS, overall survival.

impacts patient survival and immunotherapy response. In addition, we assume that MCM2 expression could predict the levels of immune cell infiltration and might be a new avenue for immune therapy in NB.

In our study, we simultaneously used mRNA and protein expression data to address the association of the MCM2-based model associated with clinical outcomes. There were to the maximum extent consistency between the two kinds of molecular expression. We know that gene expression is complicated and involves

Table 2. Multivariable Cox regression analysis of factors associated with survival in the TARGET and GWCMC cohorts

	TARGET cohort (n = 150)		GWCMC cohort (n = 130)	
	HR (95% CI)	*P*	HR (95% CI)	*P*
OS				
MCM2-based model (high vs. low)	2.3 (1.4–4.0)	0.002	8.3 (1.6–44.5)	0.013
Age, months (≥18 vs. < 18)	2.4 (0.5–13.3)	0.301	0.8 (0.3–2.4)	0.713
INSS (Advanced vs. Early)	1.4 (0.3–5.5)	0.648	5.9 (0.7–49.6)	0.104
EFS				
MCM2-based model (high vs. low)	1.8 (1.1–3.1)	0.026	1.2 (0.5–3.2)	0.668
Age, months (≥18 vs. < 18)	5.6 (1.3–23.2)	0.019	1.3 (0.5–3.0)	0.590
INSS (Advanced vs. Early)	0.4 (0.1–1.3)	0.129	6.7 (2.2–20.5)	0.001

TARGET, Therapeutically Applicable Research to Generate Effective Treatments; GWCMC, Guangzhou Women and Children's Medical Center; MCM, minichromosome maintenance; HR, hazard ratio; CI, confidence interval; INSS, the International Neuroblastoma Staging System.

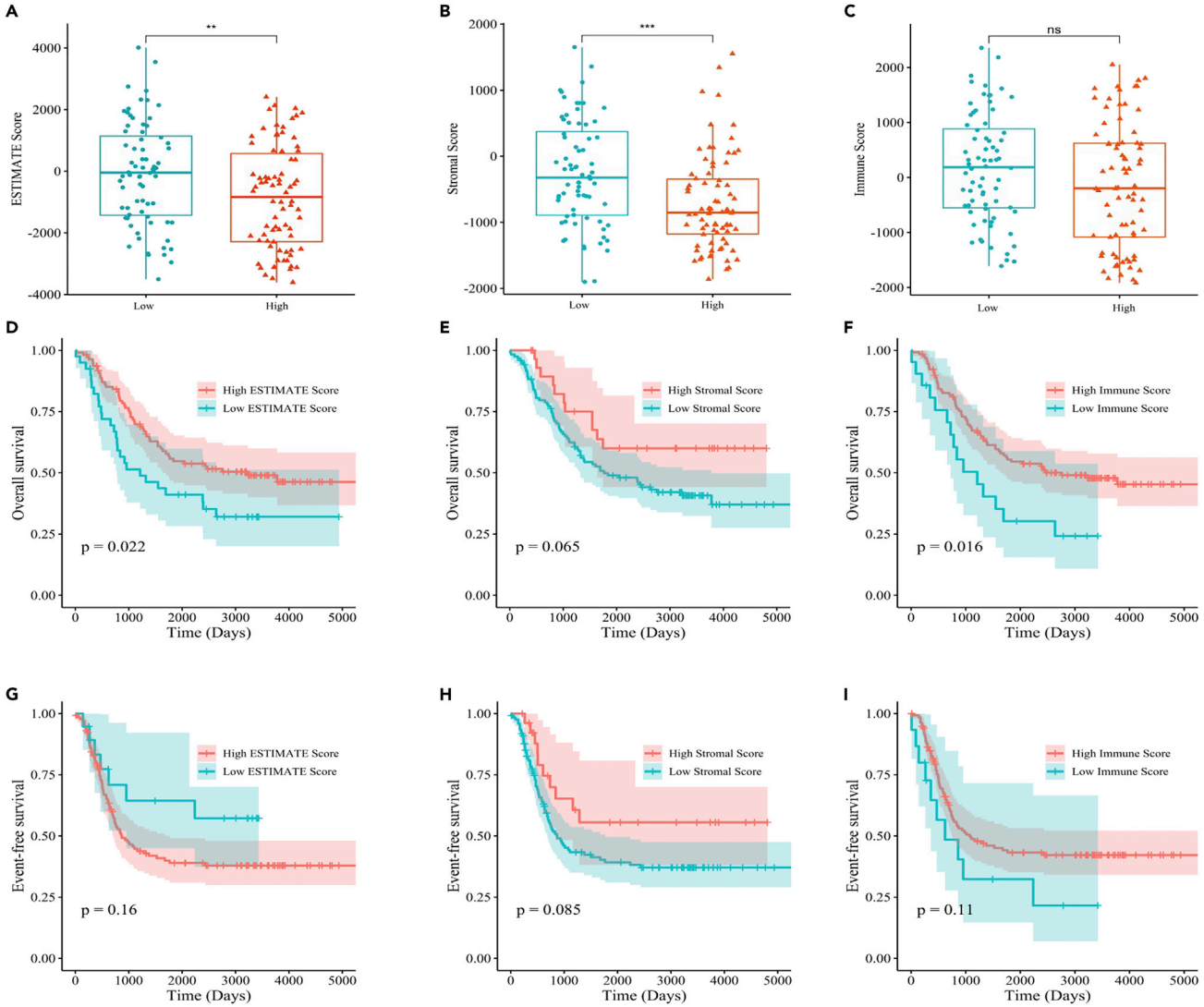

Figure 6. Relationships between ESTIMATE (A), stromal (B), and immune (C) scores and the MCM2-based risk model

OS and EFS were evaluated by the Kaplan-Meier method with the log rank test for NB patients in the TARGET dataset grouped by ESTIMATE (D for OS, G for EFS), stromal (E for OS, H for EFS), and immune (F for OS, I for EFS) scores. **p < 0.01, ***p < 0.001, ns, nonsignificant.

OS, overall survival; EFS, event-free survival; HR, hazard ratio; CI, confidence interval; MCM, minichromosome maintenance; NB, neuroblastoma.

transcription, translation, and the turnover of mRNAs and proteins. Although mRNA and protein levels undoubtedly exhibit reasonable correlation, the degree to which protein abundances and mRNA levels correlate with each other remains an intensely debated topic. Thus, both technical challenges in quantifying them and key features of the gene expression pathway are highlighted in understanding the correlation of mRNAs and proteins levels. For instance, a recent proteomic and transcriptomic survey of 375 cell lines showed that mRNAs outperformed proteins in determining the origin of cell lines.[24] More importantly, another study[25] found that differences across- and within-gene expression existed. On the one hand, across-gene expression analyses have revealed a substantial correlation between mRNA and protein levels in all kinds of life. On the other hand, within-gene correlation studies have unveiled significant but modest correlations between mRNA and protein levels for most genes. Selbach et al. pointed out that the gene expression pathway is hierarchical, indicating that protein synthesis requires the presence of an mRNA template. Hence, the degree to which protein expression can be regulated depends on the activity of the corresponding mRNA levels.[26] In view of the aforementioned considerations, the mRNA and protein levels keep consistent to some extent.

In conclusion, based on the TARGET data and our data, we confirmed the prognostic role of MCM2/5/6 expression and further developed a MCM2-based risk model for assessing patient survival that performed better than INSS and age alone. This MCM2-based risk model highlights the role of MCM2 and is a promising tool to optimize decision-making for individual NB patients.

Limitations of the study

Admittedly, a potential limitation of the current study is that further elaborate investigations *in vivo* and *in vitro* are needed to clarify how MCM2 regulates certain immune cells, which may fully explain the inner mechanisms for MCM2-based immune therapy in NB. Also, integrating multiomics datasets holds promise for understanding the complicated mechanisms and pathways underlying gene expression.

STAR★METHODS

Detailed methods are provided in the online version of this paper and include the following:

- KEY RESOURCES TABLE
- RESOURCE AVAILABILITY
  - Lead contact
  - Materials availability
  - Data and code availability
- EXPERIMENTAL MODEL AND SUBJECT DETAILS
  - Public dataset
  - GWCMC cohort
- METHOD DETAILS
  - Immunohistochemistry
  - Computational image analysis
  - Cut-off values for high and low expression
  - MCM2-based model construction
  - Estimation of immune, stromal and ESTIMATE scores
- QUANTIFICATION AND STATISTICAL ANALYSIS

SUPPLEMENTAL INFORMATION

Supplemental information can be found online at https://doi.org/10.1016/j.isci.2023.105974.

ACKNOWLEDGMENTS

This work was partially supported by the start-up program of Guangzhou Women and Children's Medical Center (No. 3001151-04). We would like to thank Senior engineer Wei Wang (Cellsvision [Guangzhou, China]) Medical Technology Inc. China) for the professional image scanning for this study.

AUTHOR CONTRIBUTIONS

Conceptualization, H.Y.W and L.Z; Supervision, H.Y.W and L.Z; Funding acquisition, H.Y.W and L.Z; Investigation, L.Z and K.C; Resources, L.Z, H.X, K.C, L.J.Q, M.L, and L.M; Methodology, H.Y.W, X.Y.L, K.L, J.F, and H.X; Writing – Original Draft, H.Y.W, L.Z, X.Y.L, and H.X; Writing – Review & Editing, H.Y.W, L.Z, X.Y.L, and H.X.

DECLARATION OF INTERESTS

The authors declare no conflicts of interest.

Received: July 14, 2022
Revised: October 7, 2022
Accepted: January 10, 2023
Published: February 17, 2023

REFERENCES

1. Maris, J.M., Hogarty, M.D., Bagatell, R., and Cohn, S.L. (2007). Neuroblastoma. Lancet *369*, 2106–2120. https://doi.org/10.1016/S0140-6736(07)60983-0.

2. Matthay, K.K., Maris, J.M., Schleiermacher, G., Nakagawara, A., Mackall, C.L., Diller, L., and Weiss, W.A. (2016). Neuroblastoma. Nat. Rev. Dis. Prim. *2*, 16078. https://doi.org/10.1038/nrdp.2016.78.

3. Ladenstein, R., Pötschger, U., Pearson, A.D.J., Brock, P., Luksch, R., Castel, V., Yaniv, I., Papadakis, V., Laureys, G., Malis, J., et al. (2017). Busulfan and melphalan versus carboplatin, etoposide, and melphalan as high-dose chemotherapy for high-risk neuroblastoma (HR-NBL1/SIOPEN): an international, randomised, multi-arm, open-label, phase 3 trial. Lancet Oncol. *18*, 500–514. https://doi.org/10.1016/S1470-2045(17)30070-0.

4. Valteau-Couanet, D., Le Deley, M.C., Bergeron, C., Ducassou, S., Michon, J., Rubie, H., Le Teuff, G., Coze, C., Plantaz, D., Sirvent, N., et al. (2014). Long-term results of the combination of the N7 induction chemotherapy and the busulfan-melphalan high dose chemotherapy. Pediatr. Blood Cancer *61*, 977–981. https://doi.org/10.1002/pbc.24713.

5. Zeng, T., Guan, Y., Li, Y.K., Wu, Q., Tang, X.J., Zeng, X., Ling, H., and Zou, J. (2021). The DNA replication regulator MCM6: an emerging cancer biomarker and target. Clin. Chim. Acta *517*, 92–98. https://doi.org/10.1016/j.cca.2021.02.005.

6. Noseda, M., and Karsan, A. (2006). Notch and minichromosome maintenance (MCM) proteins: integration of two ancestral pathways in cell cycle control. Cell Cycle *5*, 2704–2709. https://doi.org/10.4161/cc.5.23.3515.

7. Razavi, S.M., Jafari, M., Heidarpoor, M., and Khalesi, S. (2015). Minichromosome maintenance-2 (MCM2) expression differentiates oral squamous cell carcinoma from pre-cancerous lesions. Malays. J. Pathol. *37*, 253–258.

8. Amaro Filho, S.M., Nuovo, G.J., Cunha, C.B., Ramos Pereira, L.d.O., Oliveira-Silva, M., Russomano, F., Pires, A., and Nicol, A.F. (2014). Correlation of MCM2 detection with stage and virology of cervical cancer. Int. J. Biol. Markers *29*, e363–e371. https://doi.org/10.5301/jbm.5000081.

9. Honeycutt, K.A., Chen, Z., Koster, M.I., Miers, M., Nuchtern, J., Hicks, J., Roop, D.R., and Shohet, J.M. (2006). Deregulated minichromosomal maintenance protein MCM7 contributes to oncogene driven tumorigenesis. Oncogene *25*, 4027–4032. https://doi.org/10.1038/sj.onc.1209435.

10. Chang, H.H., Tseng, Y.F., Lu, M.Y., Yang, Y.L., Chou, S.W., Lin, D.T., Lin, K.H., Jou, S.T., Hsu, W.M., and Jeng, Y.M. (2020). MYCN RNA levels determined by quantitative in situ hybridization is better than MYCN gene dosages in predicting the prognosis of neuroblastoma patients. Mod. Pathol. *33*, 531–540. https://doi.org/10.1038/s41379-019-0410-x.

11. Gou, K., Liu, J., Feng, X., Li, H., Yuan, Y., and Xing, C. (2018). Expression of minichromosome maintenance proteins (MCM) and cancer prognosis: a meta-analysis. J. Cancer *9*, 1518–1526. https://doi.org/10.7150/jca.22691.

12. Lau, K.M., Chan, Q.K.Y., Pang, J.C.S., Li, K.K.W., Yeung, W.W., Chung, N.Y.F., Lui, P.C., Tam, Y.S., Li, H.M., Zhou, L., et al. (2010). Minichromosome maintenance proteins 2, 3 and 7 in medulloblastoma: overexpression and involvement in regulation of cell migration and invasion. Oncogene *29*, 5475–5489. https://doi.org/10.1038/onc.2010.287.

13. Quan, L., Qian, T., Cui, L., Liu, Y., Fu, L., and Si, C. (2020). Prognostic role of minichromosome maintenance family in multiple myeloma. Cancer Gene Ther. *27*, 819–829. https://doi.org/10.1038/s41417-020-0162-2.

14. Qiu, W.G., Polotskaia, A., Xiao, G., Di, L., Zhao, Y., Hu, W., Philip, J., Hendrickson, R.C., and Bargonetti, J. (2017). Identification, validation, and targeting of the mutant p53-PARP-MCM chromatin axis in triple negative breast cancer. NPJ Breast Cancer *3*, 1. https://doi.org/10.1038/s41523-016-0001-7.

15. Issac, M.S.M., Yousef, E., Tahir, M.R., and Gaboury, L.A. (2019). MCM2, MCM4, and MCM6 in breast cancer: clinical utility in diagnosis and prognosis. Neoplasia *21*, 1015–1035. https://doi.org/10.1016/j.neo.2019.07.011.

16. Garbati, P., Barbieri, R., Cangelosi, D., Zanon, C., Costa, D., Eva, A., Thellung, S., Calderoni, M., Baldini, F., Tonini, G.P., et al. (2020). MCM2 and carbonic anhydrase 9 are novel potential targets for neuroblastoma pharmacological treatment. Biomedicines *8*, 471. https://doi.org/10.3390/biomedicines8110471.

17. Hsieh, C.H., Yeh, H.N., Huang, C.T., Wang, W.H., Hsu, W.M., Huang, H.C., and Juan, H.F. (2021). BI-2536 promotes neuroblastoma cell death via minichromosome maintenance complex components 2 and 10. Pharmaceuticals *15*, 37. https://doi.org/10.3390/ph15010037.

18. Yoshihara, K., Shahmoradgoli, M., Martínez, E., Vegesna, R., Kim, H., Torres-Garcia, W., Treviño, V., Shen, H., Laird, P.W., Levine, D.A., et al. (2013). Inferring tumour purity and stromal and immune cell admixture from expression data. Nat. Commun. *4*, 2612. https://doi.org/10.1038/ncomms3612.

19. Xiang, S., Li, J., Shen, J., Zhao, Y., Wu, X., Li, M., Yang, X., Kaboli, P.J., Du, F., Zheng, Y., et al. (2021). Identification of prognostic genes in the tumor microenvironment of hepatocellular carcinoma. Front. Immunol. *12*, 653836. https://doi.org/10.3389/fimmu.2021.653836.

20. Pan, L., Fang, J., Chen, M.Y., Zhai, S.T., Zhang, B., Jiang, Z.Y., Juengpanich, S., Wang, Y.F., and Cai, X.J. (2020). Promising key genes associated with tumor microenvironments and prognosis of hepatocellular carcinoma. World J. Gastroenterol. *26*, 789–803. https://doi.org/10.3748/wjg.v26.i8.789.

21. McGranahan, N., Furness, A.J.S., Rosenthal, R., Ramskov, S., Lyngaa, R., Saini, S.K., Jamal-Hanjani, M., Wilson, G.A., Birkbak, N.J., Hiley, C.T., et al. (2016). Clonal neoantigens elicit T cell immunoreactivity and sensitivity to immune checkpoint blockade. Science *351*, 1463–1469. https://doi.org/10.1126/science.aaf1490.

22. Yuan, J., Lan, H., Huang, D., Guo, X., Liu, C., Liu, S., Zhang, P., Cheng, Y., and Xiao, S. (2022). Multi-omics analysis of MCM2 as a promising biomarker in pan-cancer. Front. Cell Dev. Biol. *10*, 852135. https://doi.org/10.3389/fcell.2022.852135.

23. Lei, Y., Wang, S., Liu, J., Yan, W., Han, P., and Tian, D. (2021). Identification of MCM family as potential therapeutic and prognostic targets for hepatocellular carcinoma based on bioinformatics and experiments. Life Sci. *272*, 119227. https://doi.org/10.1016/j.lfs.2021.119227.

24. Nusinow, D.P., Szpyt, J., Ghandi, M., Rose, C.M., McDonald, E.R., 3rd, Kalocsay, M., Jané-Valbuena, J., Gelfand, E., Schweppe, D.K., Jedrychowski, M., et al. (2020). Quantitative proteomics of the cancer cell line encyclopedia. Cell *180*, 387–402.e16. https://doi.org/10.1016/j.cell.2019.12.023.

25. Wang, D., Eraslan, B., Wieland, T., Hallström, B., Hopf, T., Zolg, D.P., Zecha, J., Asplund, A., Li, L.H., Meng, C., et al. (2019). A deep proteome and transcriptome abundance atlas of 29 healthy human tissues. Mol. Syst. Biol. *15*, e8503. https://doi.org/10.15252/msb.20188503.

26. Buccitelli, C., and Selbach, M. (2020). mRNAs, proteins and the emerging principles of gene expression control. Nat. Rev. Genet. *21*, 630–644. https://doi.org/10.1038/s41576-020-0258-4.

27. Otsu, N. (1979). A threshold selection method from gray-level histograms. IEEE Trans. Syst. Man Cybern. *9*, 62–66.

28. Yuhong Li, X.Z., and Chen, D. (2018). CSRNet: dilated convolutional neural networks for understanding the highly congested scenes. In Proceedings of the IEEE Conference on Computer Vision and Pattern Recognition (CVPR), pp. 1091–1100.

29. Brodeur, G.M., Pritchard, J., Berthold, F., Carlsen, N.L., Castel, V., Castelberry, R.P., De Bernardi, B., Evans, A.E., Favrot, M., Hedborg, F., et al. (1993). Revisions of the international criteria for neuroblastoma diagnosis, staging, and response to treatment. J. Clin. Oncol. *11*, 1466–1477. https://doi.org/10.1200/JCO.1993.11.8.1466.

30. McShane, L.M., Altman, D.G., Sauerbrei, W., Taube, S.E., Gion, M., and Clark, G.M.; Statistics Subcommittee of the NCI-EORTC

Working Group on Cancer Diagnostics (2005). Reporting recommendations for tumor marker prognostic studies (REMARK). J. Natl. Cancer Inst. *97*, 1180–1184. https://doi.org/10.1093/jnci/dji237.

31. Chen, Y., Zhao, Y., Yang, X., Ren, X., Huang, S., Gong, S., Tan, X., Li, J., He, S., Li, Y., et al. (2022). USP44 regulates irradiation-induced DNA double-strand break repair and suppresses tumorigenesis in nasopharyngeal carcinoma. Nat. Commun. *13*, 501. https://doi.org/10.1038/s41467-022-28158-2.

32. Van de Velde, L.A., Allen, E.K., Crawford, J.C., Wilson, T.L., Guy, C.S., Russier, M., Zeitler, L., Bahrami, A., Finkelstein, D., Pelletier, S., et al. (2021). Neuroblastoma Formation requires unconventional CD4 T cells and arginase-1-dependent myeloid cells. Cancer Res. *81*, 5047–5059. https://doi.org/10.1158/0008-5472.CAN-21-0691.

33. Liang, Y.L., Zhang, Y., Tan, X.R., Qiao, H., Liu, S.R., Tang, L.L., Mao, Y.P., Chen, L., Li, W.F., Zhou, G.Q., et al. (2022). A lncRNA signature associated with tumor immune heterogeneity predicts distant metastasis in locoregionally advanced nasopharyngeal carcinoma. Nat. Commun. *13*, 2996. https://doi.org/10.1038/s41467-022-30709-6.

34. Park, J.R., Kreissman, S.G., London, W.B., Naranjo, A., Cohn, S.L., Hogarty, M.D., Tenney, S.C., Haas-Kogan, D., Shaw, P.J., Kraveka, J.M., et al. (2019). Effect of tandem autologous stem cell transplant vs single transplant on event-free survival in patients with high-risk neuroblastoma: a randomized clinical trial. JAMA *322*, 746–755. https://doi.org/10.1001/jama.2019.11642.

STAR★METHODS

KEY RESOURCES TABLE

REAGENT or RESOURCE	SOURCE	IDENTIFIER
Software and Algorithms		
Otsu algorithm	Otsu[27]	https://ieeexplore.ieee.org/document/4310076
CSRNet	Li et al.[28]	https://github.com/leeyeehoo/CSRNet-pytorch
R software	R CRAN	https://cran.r-project.org/mirrors.html
Survminer R package	R CRAN	https://CRAN.R-project.org/package=survminer
glmnet package	R CRAN	https://CRAN.R-project.org/package=glmnet
ESTIMATE package	R CRAN	https://bioinformatics.mdanderson.org/estimate/index.html

RESOURCE AVAILABILITY

Lead contact

Further information and requests for resources should be directed to and will be fulfilled by the lead contact, Hai-Yun Wang (wanghy29@mail3.sysu.edu.cn).

Materials availability

This study did not generate new unique reagents.

Data and code availability

- The data including image and clinicopathological information generated in this study are available upon request from the lead contact or within the article and its supplementary data files.
- This study did not generate original code.
- Any additional information required to reanalyze the data reported in this paper is available from the lead contact upon reasonable request.

EXPERIMENTAL MODEL AND SUBJECT DETAILS

Public dataset

The RNA sequencing data of 150 NB samples were available from the Therapeutically Applicable Research to Generate Effective Treatments (TARGET) database (https://target-data.nci.nih.gov/Public/NBL/mRNA-seq/, accession: TARGET_NB). The data were processed by a normalization method that calculates transcripts per million (TPM) and were used as the training cohort. The corresponding clinical data collected included age at diagnosis, INSS, and MYCN amplification status.

GWCMC cohort

The formalin-fixed paraffin-embedded (FFPE) tissue samples of 130 NB patients were obtained from the Guangzhou Women and Children's Medical Center (GWCMC, Guangzhou, China) between August 2016 and December 2020. The ethical statement was approved by the Institutional Ethics Committee of the GWCMC and was in line with the ethical standards of the World Medical Association Declaration of Helsinki ([2021]078A01). All diagnoses were pathologically confirmed and restaged according to the INSS criteria.[29] The Children's Oncology Group (COG) risk classification was performed for each patient according to medical records. Parents of all NB patients provided written informed consent for participation in the study, mostly at the time of admission to the GWCMC. This study is reported according to REMARK guidelines.[30]

METHOD DETAILS

Immunohistochemistry

Three MCM proteins, namely, MCM2/5/6, were selected for immunohistochemistry (IHC) staining. In brief, pathological sequential slides at 4 μm thickness were sectioned from FFPE tumor blocks and were further deparaffinized and rehydrated. Next, endogenous peroxidase activity was blocked with 3% hydrogen peroxide for 10 min at room temperature. After antigen retrieval, the slides were incubated with primary antibodies and labeled with anti-mouse/rabbit secondary antibody (Dako REAL EnVision Detection System) for 30 min at 37°C, followed by a 3 min incubation in diaminobenzidine solution for protein detection.[31] The primary antibodies used were anti-MCM2 (ab4461, 1:1600; Abcam, Cambridge, UK), anti-MCM5 (ab17967, 1:1000; Abcam, Cambridge, UK), and anti-MCM6 antibodies (ab190948, 1:800; Abcam, Cambridge, UK).

Computational image analysis

Glass slides of IHC-stained tissue samples with good staining quality were scanned at a high resolution of 0.24 μm/pixel (Pannaromic Scan 150, 3DHistech, Hungary). All pathological images with the automated cell nucleus counting system is described as follows. First, we obtained the valid area of a whole-slide image (WSI) using the Otsu algorithm,[27] after which we cropped the WSI into 512 × 512 image patches at 40× magnification in the manner of a sliding window within the valid area. Next, each patch image was input into a trained nucleus detection model, which outputs a corresponding probability map, followed by filtered with a predefined threshold, and a set of detection points was obtained. For each detection point, we computed the mean value of the haematoxylin-eosin-DAB (HED) channel in a 5 × 5 local field. Finally, a trained logistic regression (LR) model was used to classify each detection point into a positive cell or a negative cell. The final quantification of the WSI is the sum of the count for all image patches.

In addition, to train the nucleus detection model, two professional pathologists (L. Z. and K. C.) annotated 20 WSIs for the three markers, MCM2/5/6, with a total of 31,134 points, including 16,407 positive and 14,727 negative tumor cells. We cropped ROIs containing the annotated points into 512 × 512 image patches. We chose CSRNet[28] as the cell nucleus detection model, which was used to locate nuclear positions rather than to distinguish cell types.

Cut-off values for high and low expression

The "Survminer" package in R software (version 4.1.2) was applied to calculate optimal cut-off values to define high or low expression of MCM2/5/6 using OS as the outcome. Each patient was given a binary score based on the cut-off values, with 0 for low expression and 1 for high expression, for each marker.

MCM2-based model construction

We carried out a penalized Cox regression model to select the most powerful prognostic features of the three biomarkers and clinical features[32] and then constructed an MCM-based model for predicting survival in the training cohort. The "glmnet" package was employed to perform least absolute shrinkage and selection operator (LASSO) Cox regression analysis.[33] Ten-time cross validation with *Lambda.min* criteria was used to determine optimal values of λ, and a value of $\lambda = 0.04381$ with $\log(\lambda) = -3.127893$ was chosen. Based on this value, MCM2, age and INSS were selected to construct the prediction risk model with coefficients weighted by the penalized Cox model in the training cohort. We then grouped the NB patients into low- and high-risk groups based on the model score.

Estimation of immune, stromal and ESTIMATE scores

The infiltration levels of stromal and immune components were assessed in the 150 NB samples using the "ESTIMATE" package (https://R-Forge.R-project.org/projects/estimate/) of R software.[18] A higher stromal or immune score represents a larger ratio of the corresponding component in the TME.

QUANTIFICATION AND STATISTICAL ANALYSIS

The primary outcome was OS, and the secondary outcome was EFS, as identified through medical records. OS was calculated from the date of cancer diagnosis to the date of death from any cause. EFS was calculated from the date of cancer diagnosis to the first occurrence of any event (i.e., relapse at any site, progressive disease, second malignancy, or death). Patients without an event were censored on the date of the last contact.[34]

Correlations between the expression levels of MCM2/5/6, clinical variables and the risk model were analyzed using the $\chi 2$ test or Fisher exact test. We applied Kaplan–Meier curves with the log rank test to estimate differences in OS and EFS between patients with high and low expression of the three markers and the risk model. Multivariable Cox regression analysis and hazard ratios (HRs) with 95% confidence intervals (CIs) with backwards selection were then utilized to assess the prognostic roles of these different factors, with mutual adjustment for one another. Finally, we compared the sensitivity and specificity of MCM2, age, INSS and the risk model for prognosis prediction using a receiver operating characteristic (ROC) curve and the area under the curve (AUC).

Statistical analyses were performed using RStudio (version 4.1.2, Inc., Boston, MA), GraphPad Prism 7 (GraphPad Software, La Jolla, CA, USA), and Stata version 15.1 (TX, USA). All statistical tests were two-sided; the results were considered significant at a p value less than 0.05.